Analysing cyclic well behaviour via time series analytics and reservoir simulation

Paul Michael B. Abrasaldo, Sadiq J. Zarrouk, and Andreas W. Kempa-Liehr

Department of Engineering Sciences, The University of Auckland, Private Bag 92019, Auckland, New Zealand

pabr612@aucklanduni.ac.nz

Keywords: *Geothermal energy, machine learning, feature engineering, time-series analytics, fractional dimension, reservoir modelling*

ABSTRACT

The geothermal energy industry has always been in constant flux with the advent of new technology and the rich experience of long-time geothermal operators. However, the industry's growth has been tempered by the inherent risks associated with geothermal energy extraction, particularly by unfavourable drilling outcomes. In this study, we looked at the characteristics of a low permeability geothermal production well exhibiting weak discharge metrics relative to other nearby wells. Fluctuations in the maximum discharge pressure of the target well have caused interruptions in its utilisation resulting in additional costs and downtime for the geothermal operator.

The performance of the target well was analysed using sensor data from the surface facility, and a workflow based on systematic time-series feature engineering for improved utilisation of the well was proposed. A predictive model was trained using the extracted time-series features and evaluated to forecast the occurrence of low discharge pressure events in the target well. The same dataset was then used to develop a reservoir model that captured the behaviour of the target well observed during post-drilling completion tests and while producing into the surface facility.

1. INTRODUCTION

The pace of growth of geothermal energy production has slowed down since it peaked in the mid-1980s (Huttrer, 2021). The abundance of cheaper alternatives has negatively impacted the adoption of geothermal energy, especially in emerging economies (Winters & Cawvey, 2015). Furthermore, high uncertainty in well drilling outcomes due to resource heterogeneity may have further driven negative investor opinion on geothermal technology (Witkin, 2009).

1.1 Low discharge pressure events (LDPEs)

Industrial experience worldwide has shown that it is fairly common to see low permeability or weak production wells drilled near good producers (Aragon-Aguilar et al., 2017). This occurrence is also a result of the heterogeneous nature of most geothermal reservoirs. In the case of the target area for this study, the resulting arrangement of production wells on the surface (Figure 1) gives rise to operational challenges that may result in a loss of revenue due to well outages and additional costs from well intervention activities. A single two-phase header is shared by the target low permeability wells and multiple high permeability wells on the same well pad. Most of the time, the target well can operate normally, even though it is at a lower wellhead pressure than the other nearby wells as long as it is marginally higher than the two-phase header pressure. However, the cyclic behaviour of the target well results in its maximum discharge pressure (MDP) fluctuating around the required operating pressure dictated by the pipe network. Haukawa and O'Sullivan (1982) and Grant and Bixley (2011) have looked at similar instabilities in well discharge behaviour in the past.

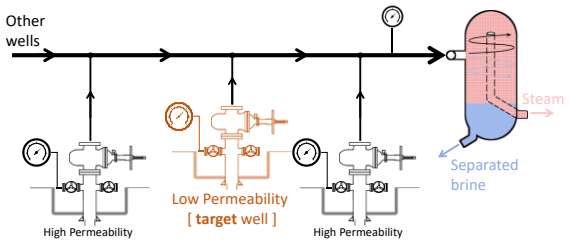

Figure 1. Schematic diagram of the surface facilities in the vicinity of the target well.

During the periods when the MDP of the target well falls below the minimum pressure required by the system, the tendency is for the well to stop producing altogether. Such cases usually result in the geothermal operator incurring additional costs to revive the well, notwithstanding the lost revenue due to well downtime. Reliably predicting these low discharge pressure events can allow the operator to conduct preventive measures that can lessen well outages and potentially avoid well stimulation costs altogether.

1.2 Field data and study objectives

The data used in this study comes from sensors installed at various points of the geothermal surface facility. In particular, this study used the wellhead pressure (WHP) of the target well as the main parameter during the development of the predictive models. Other system operating data, such as the actual pressures along the two-phase header, separated steam flow rates, and WHPs of other wells on the same pad, were also used in the analysis.

This paper aimed to develop an operational solution that would improve the overall availability of the target well. Recently established techniques in machine learning and systematic time-series feature engineering was utilised to establish a workflow to analyse and model the target LDPEs. Numerical reservoir simulations were also conducted to characterise the potential mechanisms that may drive such events in low permeability wells.

2. FEATURE-BASED TIME-SERIES MODELLING

Any signal with time as the independent or ordering variable can be categorised as a time series (e.g., tracer recovery data, well output trends) (Box et al., 2015). This study involves the analysis of sensor data that was measured in real-time. Given the input time-series data and the labelled events, the primary task in predicting the occurrence of the LDPEs can be considered a time-series classification problem (Liao, 2005). Conventional time-series analysis is usually performed on the raw values of the input data. Still, there are instances where a feature-based approach proves to be more insightful and effectively displays the unique characteristics and dynamics contained within the time series (Kempa-Liehr et al., 2019).

ISSN 2703-4275

2.1 Systematic time-series feature engineering (STSFE)

The cumbersome process of calculating and selecting relevant time-series characteristics from the input data has already been automated and streamlined in the *tsfresh* Python library (Christ et al., 2018). The package allows for the extraction of 794 time-series features by default, and each one can be tested for statistical relevance with respect to the target using built-in univariate hypothesis testing.

WHP data of the target well, covering the period of 1 January 2019 until 30 June 2021, were used for this study. A subset of this dataset and the labelling process are shown in Figure 2 and Table 1, respectively. Periods of missing data were observed within the dataset due to sensor or network failure. However, no imputation to fill in such missing values was performed in this work. The LDPEs were identified by locating the periods wherein the WHP of the target well was lower than the measured pressure within the two-phase header. The input data were then sectioned into non-overlapping windows of varying lengths. Each window was assigned a value of 0 or 1 if a target event (LDPE) occurred within a certain look-forward interval. A transition period was manually designated after each occurrence of the target event wherein the taken measurements were considered unstable and thus excluded from the analysis.

The labelled input data are then processed using tsfresh to generate the 794 time-series features such as distribution characteristics, autocorrelation metrics, energy, entropy, and other stochasticity measures. However, time-series features extracted from highly complex systems are known to have high degrees of collinearity, and most of them would not be significant in predicting the target (Kennedy et al., 2021). Tsfesh uses the Mann-Whitney U test to estimate the relevance of binary-type time-series features, while the Kendall-Tau rank test is used for continuous features. The resulting p-values for each feature are then subjected to the Benjamini-Yekutieli procedure (Figure 3) to preserve the false-discovery rate of the selected time-series features (Benjamini & Yekutieli, 2001).

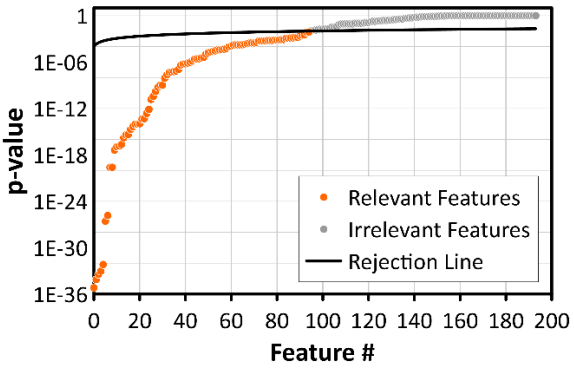

Figure 3. Calculated p-values of extracted features using univariate hypothesis testing plotted together with the Benjamini-Yekutieli rejection line.

Table 1. Example labels from three adjacent windows close to a collapse event. The labels correspond to the example shown in Figure 2.

Window No.	Timestamp	Label	Remarks
i	2019-05-28 12:00	0	No event within the look-forward interval
$i+1$	2019-05-28 18:00	0	No event within the look-forward interval
$i+2$	2019-05-29 00:00	1	Event occurred within look-forward interval

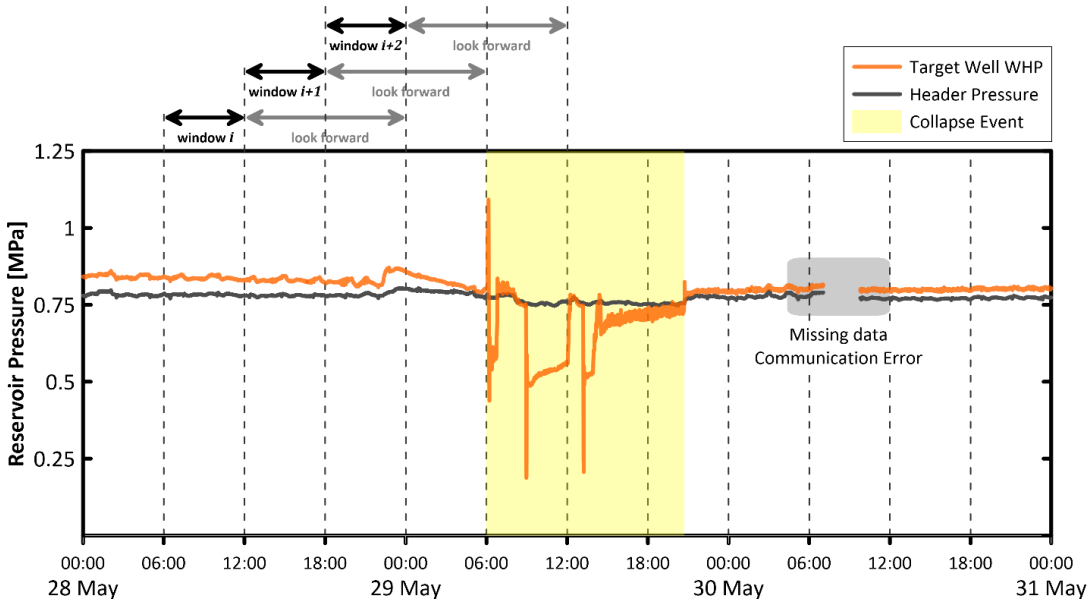

Figure 2. Wellhead and header pressure data illustrating the windowing procedure and other data handling considerations

The collinearity of the extracted features is addressed by a second feature selection step involving the multi-variate recursive feature elimination (RFE) algorithm within the scikit-learn library (Pedregosa et al., 2011). In summary, this process is done by iteratively fitting a non-linear regression algorithm, such as a Random Forest regressor, and then removing the least important feature from the set of considered features at the end of every iteration. This feature selection method was applied to the training data set only using a ten-fold cross-validation training process with three repetitions.

2.2 Classification modelling

The final set of time-series features that made it through the two-step selection process was used as the inputs to train and evaluate the predictive models. The features extracted from the first year of data were designated as the training dataset, while the rest of the data were used for evaluating the classification performance on unseen data. Random forest classifiers and lightGBM gradient-boosted decision tree (Ke et al., 2017) models were selected for evaluation in this study. The Matthews correlation coefficient (MCC) was used as the primary metric to evaluate the performance of all the models. A value of 1 for the MCC indicates a perfectly accurate model, while -1 represents a perfectly inaccurate model.

3. RESERVOIR MODELLING

A TOUGH reservoir model (Pruess, 1991) was built to study the characteristics of LDPEs in the target well. An initial model was developed to match the pressure transient behaviour of the target during its post-drilling completion test. The resulting model was then calibrated against the target well's selected production history by varying the model's fractional dimension parameter. The calibration process in both stages of numerical reservoir simulation was automated using the *pyTOUGH* (Croucher, 2011) and *scipy* (Virtanen et al., 2020) Python libraries.

The overall structure of the reservoir model (Figure 4) was adopted from the numerical framework for pressure transient analysis (PTA) developed by McLean and Zarrouk (2017). The model was first calibrated against the pressure data during the injectivity and falloff tests. The fractional dimension approach (O'Sullivan et al., 2005) to simulate flow within a fractured reservoir was selected for use in this study for its simplicity and effectiveness (Zarrouk et al., 2007). The fractional dimension parameter was adjusted, and the block volumes were recalculated at every timestep to achieve the best match against the measured pressure data and calculated pressure derivative.

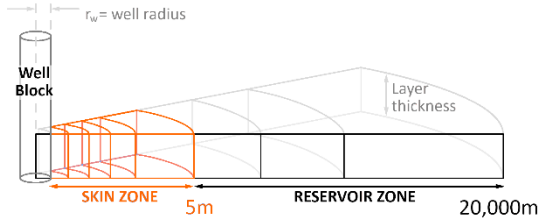

Figure 4. Grid setup for the numerical PTA and production history matching after McLean and Zarrouk (2017).

The resulting model calibrated against the transient pressure response of the target well was then used to simulate the behaviour of the same well during production. The mass flow trend of the target well was obtained by back calculating from the measured steam flows at the separator. Reservoir pressure trends associated with the target well were then generated using the WELLSIM™ wellbore simulator (Murray & Gunn, 1993). A fixed-mass generator was defined in the reservoir model based on the mass flow rate trend of the well, and the fractional dimension was again adjusted at every timestep to match the reservoir pressure values.

4. RESULTS

4.1 Predictive model

The first feature selection stage resulted in 93 statistically relevant time-series characteristics for predicting the target events (Table 2). The potential collinearity of the initial feature set was addressed in the second step using recursive feature elimination. The result of this final step is summarised in Figure 5, wherein it could be seen that the MCC of the models improved as the number of model inputs increased but started to taper off, beginning with models with seven or more variables.

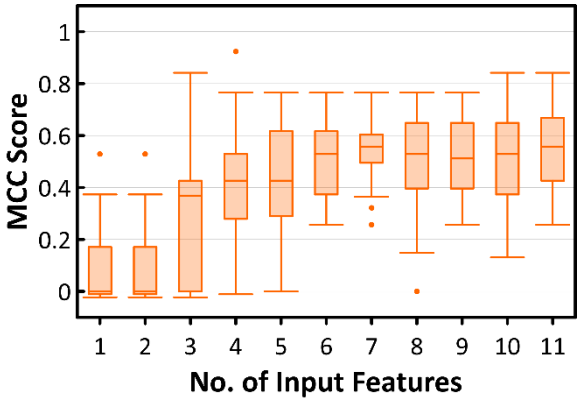

Figure 5. RFE results show model training performance levelling off for models with more than seven (7) variables.

Several explanatory features from this multi-step feature selection process are indicators of the regularity or complexity of the windowed time-series data (Figure 6). For example, approximate entropy is a statistical measure that quantifies the amount of regularity in medical datasets, such as those taken from an electrocardiogram (Pincus et al., 1991). These features indicate a significant change in the dynamics of the WHP data before an LDPE. They may point to a corresponding change in the operational state of the well driven by certain reservoir processes.

Table 2. Top explanatory time-series features from the two-stage feature selection process.

Time-series Property	*tsfresh* feature name	p-value	Description
Approximate entropy	Value__approximate_entropy__m_2__r_0.5	6.45×10^{-36}	Property that measures regularity within a time-series dataset.
	Value__approximate_entropy__m_2__r_0.3	7.71×10^{-35}	
	Value__approximate_entropy__m_2__r_0.7	9.42×10^{-34}	
Complexity-invariant distance	Value__cid_ce__normalize_True	1.47×10^{-26}	Time-series metric that measures complexity (# peaks, valleys, etc.).
Ratio beyond sigma	Value__ratio_beyond_r_sigma__r_1	4.78×10^{-14}	Ratio of values that are more than r * standard deviation away from the mean of the input time series.
Last location of maximum	Value__last_location_of_maximum	7.03×10^{-8}	Identifies the last location of the maximum value relative to the length of the input time-series
Linear trend r-value	Value__linear_trend__attr_"rvalue"'	9.74×10^{-7}	The r-value of a least-squares regression for values of a given time series.

The feature selection and model training pipeline was automated and optimised using the Optuna optimisation library (Akiba et al., 2019). The learning control parameter *lambda_*1 of the lightGBM model showed the highest importance, while an optimal false discovery rate of 0.121 for the Benjamini-Yekutieli procedure was obtained during the optimisation process. During the training phase, an MCC score of 0.68 was recorded for the best-performing model (Figure 7). Furthermore, the same model was evaluated using the validation dataset and obtained an MCC score of 0.66. The relatively small performance difference between the training and validation phase shows that the selected model is rather robust for predicting the target event and is not overfitted.

Several time-series window sizes and look-forward intervals were also tested. Using a 3-hour window size and a look-forward interval of 6 hours, the selected model correctly predicted 28 out of 33 target events in the validation dataset. Instances of false positives and negatives were mixed-in with correct predictions when observing the model validation results (Figure 8).

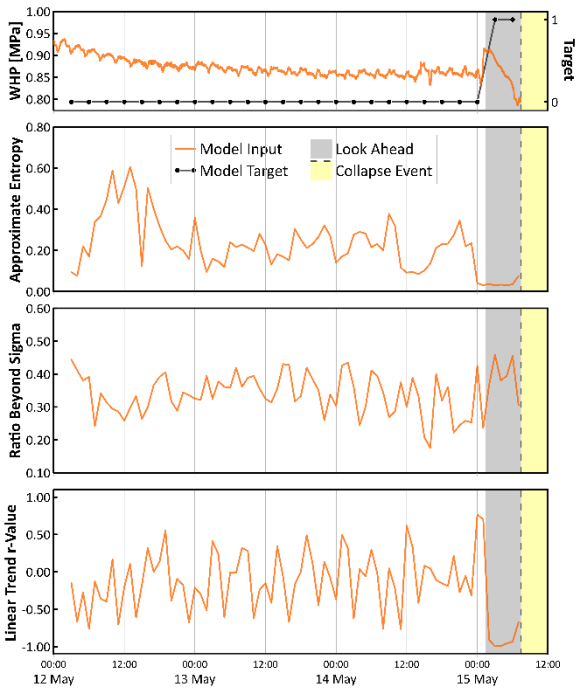

Figure 6. Change in value over time for the top explanatory time-series features.

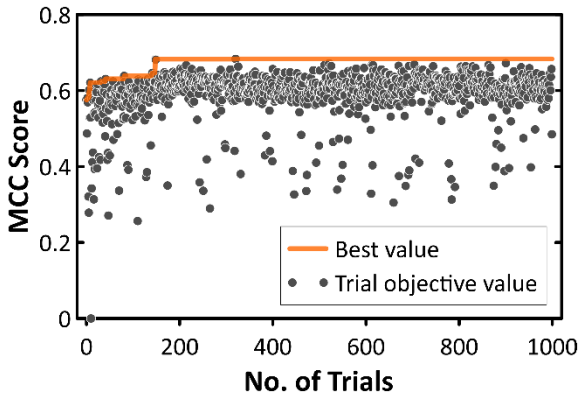

Figure 7. Optimisation history of the classifier during the training phase.

4.3 Reservoir simulation

Numerical pressure transient analysis of the falloff data of the target well resulted in a good match (Figure 9). Significant fluctuations in the resulting fractional dimension trend corresponded to noticeable oscillations in the measured pressure data. Fractional dimension fluctuations were more prominent at the start of the falloff test, with a general increasing trend in absolute value until it plateaued at a value of about 2.2. Similar behaviour in the modelled fractional dimension of a low permeability well in Belgium was also reported by Adiputro et al. (2020). The simulation results show that significant near-wellbore pressure variations directly affect the reservoir flow paths from the well feedzones.

Table 3 lists the model parameters that were modified from the reference values to match the characteristics of the target well. It can be observed that the well has negative skin, indicating no near-wellbore formation damage, but also has a relatively low reservoir permeability of 2 mD.

A WELLSIM™ wellbore model of the target well was calibrated against measured bore output and flowing survey data. The model was used to convert the WHP and mass flow time-series data into the reservoir pressure trend that will be used as reference data for production history matching. From this process, it was determined that about 2.9 MPa of reservoir pressure drawdown was needed for the MDP of the target well to fall below the desired operating condition (Figure 10).

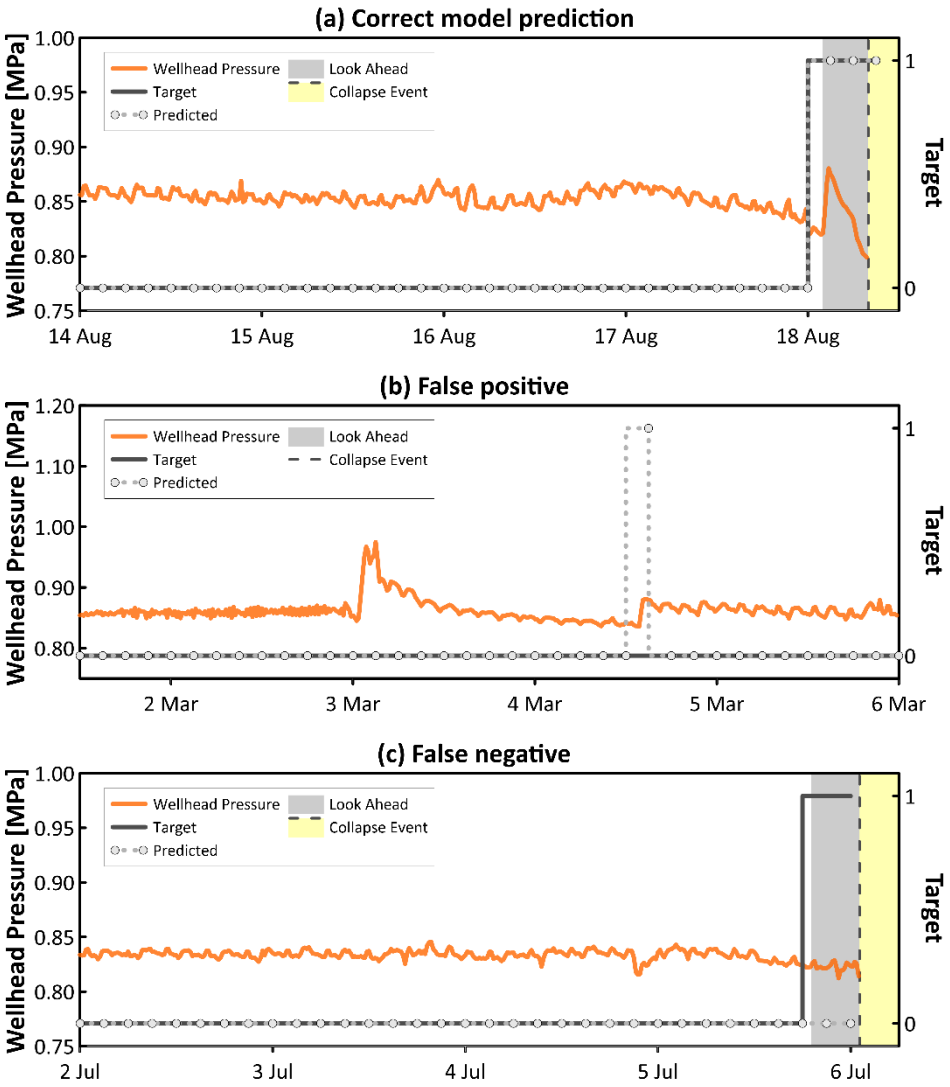

Figure 8. Sample predictions of the best-performing model showing (a) correct, (b) false positive and (c) false negative predictions.

ISSN2703-4275

Table 3. Calibrated reservoir model parameters that were modified from the reference values as established by McLean & Zarrouk (2017).

Parameter	Value used in the calibrated model	Parameter and description
Layer thickness (m)	1200	Layer thickness (m): interpreted permeable section of the reservoir intersected by the target well
Well radius (m)	0.11	Average well radius in the open section of the well
Reservoir permeability (mD)	2.0	Permeability of reservoir rock intersected by the well track
Skin factor	-2.0	A dimensionless parameter representing near-wellbore effects
Injectate temperature (°C)	45.0	Estimate of injectate temperature at the tool depth

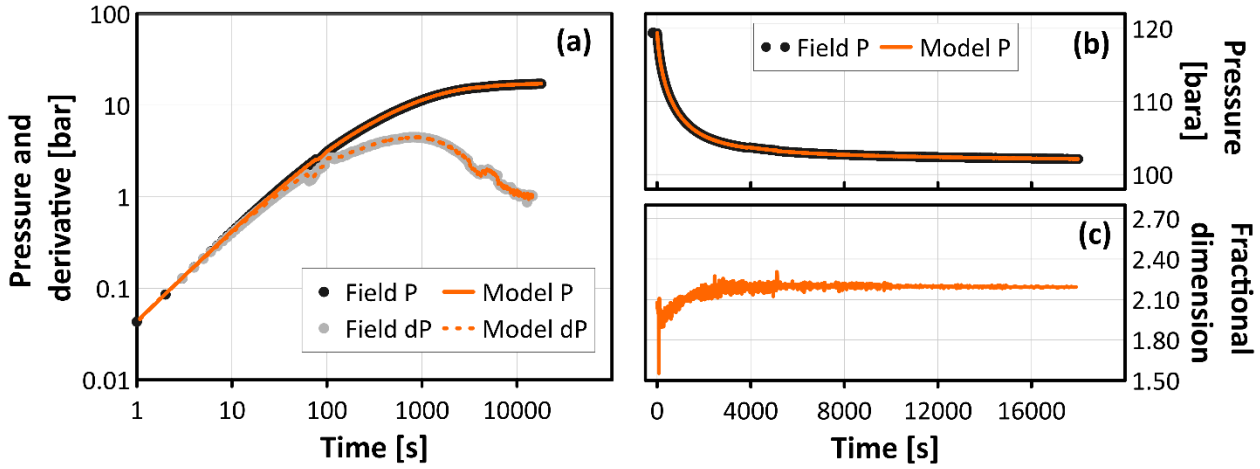

Figure 9. Numerical PTA results for the target well showing (a) pressure derivative of the field and simulated data, (b) pressure history match and (c) the resulting calibrated fractional dimension.

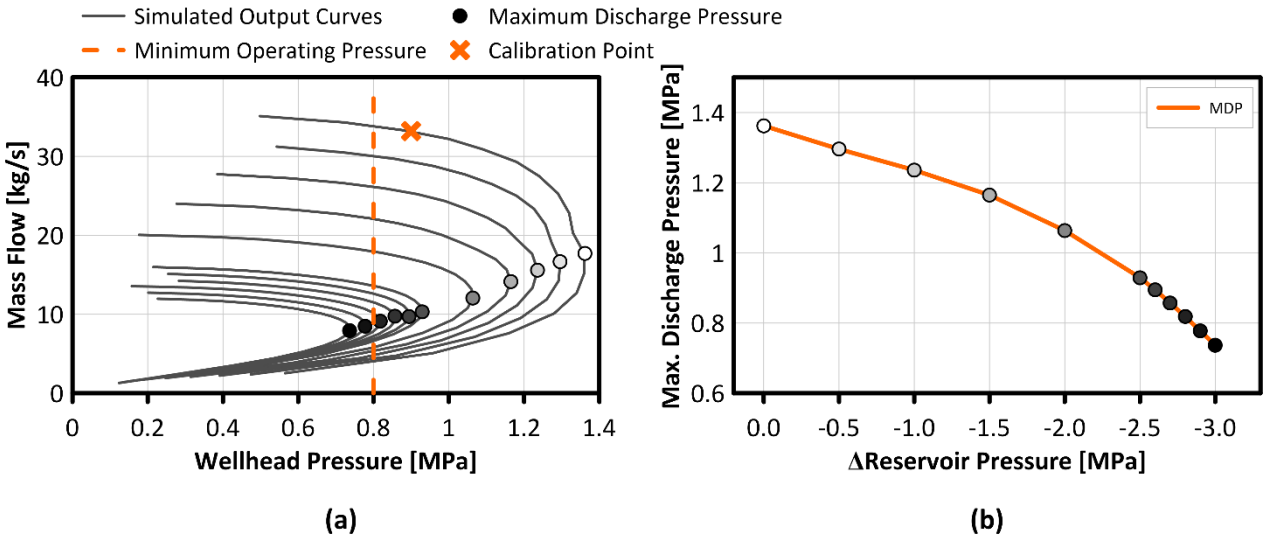

Figure 10. Wellbore simulation results of the target well showing (a) output curves at varying reservoir pressure drawdown values and (b) variation of the target well's MDP with respect to changes in reservoir pressure.

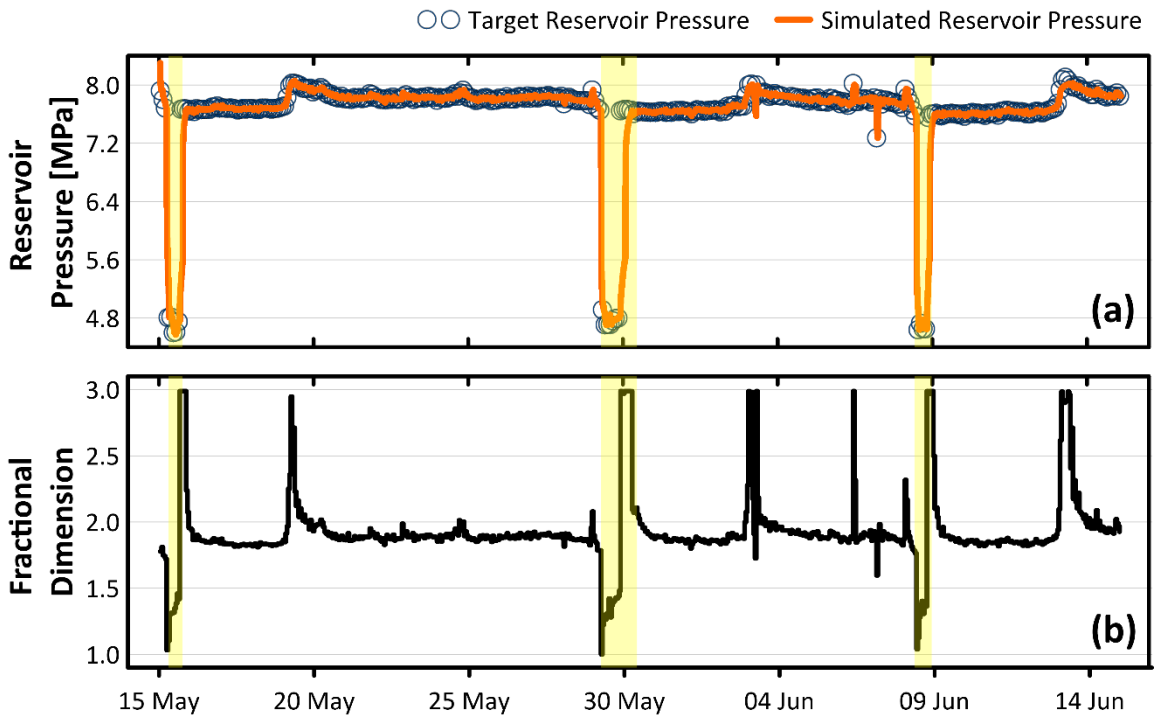

Figure 11. Historical match of reservoir pressure trend of the target well using the radial model and the resulting calibrated fractional dimension changes of the model.

The radial reservoir model was run using the mass flow rates of the target well as inputs and the reservoir pressure trend as calibrating points. A similar process of modifying the fractional dimension of the model at each timestep resulted in a good fit with the reservoir pressure trend. We can see in the calibrated fractional dimension values (Figure 11) that the model simulates a significant drop in this parameter's value during an LDPE. The fractional dimension drops to 1.0 (one-dimensional flow) when the target event occurs, then recovers to 3.0 (three-dimensional flow) as the well is taken off service to recover. It can be observed that the fractional dimension during regular operation settles at around a value of 1.85, which can be considered sub-commercial for a geothermal production well. As a reference, Zarrouk et al. (2007) stated that the fractional dimension during steady-state production for a good producer should be greater than 2.4.

5. CONCLUSION

This study has successfully applied systematic time series feature engineering and machine learning for time-series data in the geothermal industry. The objective of improving well utilisation of the target well was achieved by developing robust models that can predict the occurrence of the LDPEs ahead of time, allowing operators to minimise well downtime and avoid well stimulation costs. Furthermore, reservoir simulation also showed that the inherent low permeability of the reservoir near the well feedzone is the primary driver of the LDPEs. Improving the near-wellbore permeability of the target well is possible using existing well-enhancement methods. Still, it would require an in-depth analysis of the potential output gain to determine the economic viability of such activity.

ACKNOWLEDGEMENTS

The authors would like to express their appreciation to the New Zealand Ministry of Business, Innovation and Employment (MBIE) for their financial support through the Empowering Geothermal Energy funds and Energy Development Corporation (EDC) for providing access to the well data used for this study.

REFERENCES

Adiputro, A. S., Zarrouk, S. J., Clarke, R. J., Harcouet-Menou, V., & Bos, S. (2020). Geothermal wells with water hammer during injection falloff test: Numerical pressure transient analysis. *Geothermics*.

Akiba, T., Sano, S., Yanase, T., Ohta, T., & Koyama, M. (2019). Optuna: A Next-generation Hyperparameter Optimization Framework. *Proceedings of the 25th ACM SIGKDD International Conference on Knowledge Discovery & Data Mining* (pp. 2523-2631). Anchorage, AK, USA: Association for Computing Machinery.

Aragon-Aguilar, A., Izquierdo-Montalvo, G., Lopez-Blanco, S., & Arellano-Gomez, V. (2017). Analysis of heterogeneous characteristics in a geothermal area with low permeability and high temperature. *Geoscience Frontiers*, 1039-1050.

Benjamini, Y., & Yekutieli, D. (2001). The control of the false discovery rate in multiple testing under dependency. *Ann. Statist.*, 1165-1188.

Box, G. E., Jenkins, G. M., Reinsel, G. C., & Ljung, G. M. (2015). *Time Series Analysis: Forecasting and*

Control. Hoboken, New Jersey: John Wiley & Sons.

Christ, M., Braun, N., Neuffer, J., & Kempa-Liehr, A. W. (2018). Time Series FeatuRe Extraction on basis of Scalable Hypothesis tests (tsfresh – A Python package). *Neurocomputing*, 72-77.

Croucher, A. E. (2011). Pytough: a python scripting library for automating tough2 simulations. *New Zealand Geothermal Workshop.* Auckland, New Zealand.

Grant, M. A., & Bixley, P. F. (2011). Chapter 8 - Production Testing. In M. A. Grant, & P. F. Bixley, *Geothermal Reservoir Engineering (Second Edition)* (pp. 131-168). Academic Press.

Haukwa, C. B., & O'Sullivan, M. J. (1982). A Study of Cycling in Geothermal Wells. *Proceedings of the New Zealand Geothermal Workshop* (pp. 425-431). Auckland, New Zealand: University of Auckland Geothermal Institute.

Huttrer, G. W. (2021). Geothermal Power Generation in the World 2015-2020 Update Report. *Proceedings World Geothermal Congress 2020+1*. Reykjavik, Iceland.

Ke, G., Meng, Q., Finley, T., Wang, T., Chen, W., Ma, W., . . . Liu, T.-Y. (2017). LightGBM: A Highly Efficient Gradient Boosting Decision Tree. *Advances in Neural Information Processing Systems 30*, (pp. 3149-3157).

Kempa-Liehr, A. W., Oram, J., Wong, A., Finch, M., & Besier, T. (2019). Feature Engineering Workflow for Activity Recognition from Synchronised Inertial Measurement Units. *Asian Conference on Pattern Recognition* (pp. 223-231). Auckland, New Zealand: Springer.

Kennedy, A., Nash, G., Rattenbury, N., & Kempa-Liehr, A. (2021). Modelling the projected separation of microlensing events using. *Astronomy and Computing*.

Liao, T. (2005). Clustering of time series data—a survey. *Pattern Recognition*, 1857-1874.

McLean, K., & Zarrouk, S. J. (2017). Pressure transient analysis of geothermal wells: A framework for numerical modelling. *Renewable Energy*, 737-746.

Murray, L., & Gunn, C. (1993). Toward integrated geothermal reservoir and wellbore simulation: TETRAD and WELLSIM. *Proceedings of the 15th New Zealand Geothermal Workshop.*

O'Sullivan, M. J., Croucher, A. E., Anderson, E. B., Kikuchi, T., & Nakagome, O. (2005). An Automated Well-Test Analysis System (AWTAS). *Geothermics*, 3-25.

Pedregosa, F., Varoquaux, G., Gramfort, A., Michel, V., Thirion, B., Grisel, O., . . . Duchesnay, E. (2011). Scikit-learn: Machine Learning in Python. *Journal of Machine Learning Research*, 2825-2830.

Pruess, K. (1991). *TOUGH2—A general-purpose numerical simulator for multiphase fluid and heat flow.* Berkeley, CA, USA: Lawrence Berkeley Laboratory.

Virtanen, P., Gommers, R., Oliphant, T. E., Haberland, M., Reddy, T., Cournapeau, D., . . . Millman, K. J. (2020). SciPy 1.0: Fundamental Algorithms for Scientific Computing in Python. *Nature Methods*, 261-272.

Winters, M. S., & Cawvey, M. (2015). Governance Obstacles to Geothermal Energy Development in Indonesia. *Journal of Current Southeast Asian Affairs, 34*(1), 27-56.

Witkin, J. (2009, 10 November). *Financial Challenges for Geothermal Power*. Retrieved from The New York Times: https://green.blogs.nytimes.com/2009/11/10/financing-challenges-for-geothermal-power/

Zarrouk, S. J., O'Sullivan, M., Croucher, A., & Mannington, W. (2007). Numerical modelling of production from the Poihipi dry steam zone: Wairakei geothermal system, New Zealand. *Geothermics*, 289-303.

ISSN2703-4275